Plant Physiology and Biochemistry 106 (2016) 228–235

Contents lists available at ScienceDirect

Plant Physiology and Biochemistry

journal homepage: www.elsevier.com/locate/plaphy

Research article

Superoxide generated from the glutathione-mediated reduction of selenite damages the iron-sulfur cluster of chloroplastic ferredoxin

Brian Fisher [a], Dmitry Yarmolinsky [b, 1], Salah Abdel-Ghany [c, 2], Marinus Pilon [c], Elizabeth A. Pilon-Smits [c], Moshe Sagi [b], Doug Van Hoewyk [a, *, 3]

[a] Coastal Carolina University, Biology Department, Conway, SC, 29526, USA
[b] Ben-Gurion University, Blaustein Institutes for Desert Research, Beer Sheva, Israel
[c] Colorado State University, Biology Department, Fort Collins, CO, 80523, USA

ARTICLE INFO

Article history:
Received 8 February 2016
Received in revised form
4 May 2016
Accepted 5 May 2016
Available online 9 May 2016

Keywords:
Iron-sulfur cluster
Selenium
Oxidative stress
Ferredoxin
Superoxide

ABSTRACT

Selenium assimilation in plants is facilitated by several enzymes that participate in the transport and assimilation of sulfate. Manipulation of genes that function in sulfur metabolism dramatically affects selenium toxicity and accumulation. However, it has been proposed that selenite is not reduced by sulfite reductase. Instead, selenite can be non-enzymatically reduced by glutathione, generating selenodiglutathione and superoxide. The damaging effects of superoxide on iron-sulfur clusters in cytosolic and mitochondrial proteins are well known. However, it is unknown if superoxide damages chloroplastic iron-sulfur proteins. The goals of this study were twofold: to determine whether decreased activity of sulfite reductase impacts selenium tolerance in Arabidopsis, and to determine if superoxide generated from the glutathione-mediated reduction of selenite damages the iron-sulfur cluster of ferredoxin. Our data demonstrate that knockdown of sulfite reductase in Arabidopsis does not affect selenite tolerance or selenium accumulation. Additionally, we provide *in vitro* evidence that the non-enzymatic reduction of selenite damages the iron-sulfur cluster of ferredoxin, a plastidial protein that is an essential component of the photosynthetic light reactions. Damage to ferredoxin's iron-sulfur cluster was associated with formation of apo-ferredoxin and impaired activity. We conclude that if superoxide damages iron-sulfur clusters of ferredoxin *in planta*, then it might contribute to photosynthetic impairment often associated with abiotic stress, including toxic levels of selenium.

1. Introduction

Plants can accumulate and metabolize selenium (Se), but do not require it as a trace element, in contrast to some algae, many bacteria, and animals (Pilon-Smits and Quinn, 2010). Selenium metabolism in plants has nutritional significance for consumers, including humans, whose worldwide Se requirement is provided primarily through a plant-based diet (Rayman, 2000). Se is chemically similar to sulfur (S), and the uptake and reduction of inorganic Se is mediated by transporters and enzymes involved in the S assimilation pathway, as reviewed elsewhere (Zhu et al., 2009).

Arabidopsis plants with mutations in sulfate transporters and sulfur assimilatory enzymes have played a significant role in our understanding of pathways involved in Se uptake and metabolism. For example, mutation in the sulfate transporter (*SULTR1;2*) increased tolerance to selenate 6-fold compared to wildtype (WT) plants, which was explained by restricting the amount of selenate transported into roots (El Kassis et al., 2007). Once selenate is transported into plant cells, its reduction likely occurs predominantly in plastids where it is metabolized by S assimilatory enzymes. The rate-limiting step of selenate reduction is controlled by ATP-sulfurylase, which hydrolyzes ATP and couples AMP to sulfate, and presumably to selenate as well (Dilworth and Bandurski, 1977). Overexpression of *ATPS1* increased the reduction of selenate almost

* Corresponding author.
E-mail addresses: bjfisher@g.coastal.edu (B. Fisher), dmitry.yarmolinsky@ut.ee (D. Yarmolinsky), salahghany@gmail.com (S. Abdel-Ghany), pilon@colostate.edu (M. Pilon), epsmits@colostate.edu (E.A. Pilon-Smits), gizi@bgu.ac.il (M. Sagi), dougvh@coastal.edu (D. Van Hoewyk).
[1] Present address: University of Tartu, Institute of Technology, Tartu, Estonia.
[2] Permanent address: Zagazig University, Faculty of Science, Botany Department, Zagazig 44519, Egypt.
[3] Present address: Ankara University, Biotechnology Institute, Tandoğan Campus, 06110 Ankara, Turkey.

http://dx.doi.org/10.1016/j.plaphy.2016.05.004
0981-9428/

3-fold, resulting in increased selenate tolerance and Se accumulation (Pilon-Smits et al., 1999; Sors et al., 2005). Furthermore, mutation of *APR2*, the enzyme that catalyzes the formation of sulfite from phosphorylated sulfate, decreased selenate tolerance 2.5-fold, and coincided with increased levels of selenate and total Se compared to WT plants (Grant et al., 2011). In summary, altered expression of genes participating in sulfate uptake and reduction results in concomitant changes in Se tolerance and accumulation.

Sulfite reductase (SiR)-the enzyme that catalyzes the reaction of sulfite to sulfide-is a rate-limiting enzyme in the sulfate assimilation pathway (Khan et al., 2010) and is capable of alleviating sulfite toxicity (Yarmolinsky et al., 2013). It is not known whether altered SiR expression affects Se tolerance and accumulation in plants. While enzymes involved in sulfur metabolism are generally assumed to metabolize Se analogs, SiR may not be important for selenite reduction and detoxification. In a study that compared the incorporation of radioactive sulfite and selenite into cysteine and selenocysteine, respectively, two pieces of evidence emerged suggesting that sulfite and selenite reduction occur *via* two independent pathways (Ng and Anderson, 1979). Cyanide, a potent SiR inhibitor, blocked sulfite's incorporation into cysteine, but had no effect on the incorporation of selenite into selenocysteine. This suggests that plant SiR is not a selenite reductase, as similarly reported for *Escherichia coli* SiR (Turner et al., 1998). Secondly, the *in-vitro* incorporation of selenite into selenocysteine was dependent upon the reductant glutathione (GSH).

Because of these findings, it has been proposed that selenite reduction in plants and other organisms is mainly non-enzymatic and mediated by GSH (Ng and Anderson, 1979; Kessi and Hanselmann, 2004). Indeed, depletion of internal GSH in *Rhodobacter rubrum* and *Rhodobacter capsulatus* decreased selenite reduction (Kessi, 2006). *In-vitro* evidence demonstrated that non-enzymatic reduction of selenite by GSH rapidly yields selenodiglutathione and superoxide (Seko et al., 1989; Kessi and Hanselmann, 2004; Chen et al., 2007). Additionally, *in vivo* studies using human cells (Wallenberg et al., 2010), Arabidopsis (Grant et al., 2011), and the green alga *Chlamydomonas reinhardti* (Vallentine et al., 2014) also demonstrate that selenite treatment produces toxic levels of superoxide. Superoxide is a reactive oxygen species (ROS) that can induce oxidative stress by oxidizing and impairing protein structure. For example, iron-sulfur (Fe–S) clusters present as cofactors in various Fe–S proteins (Balk and Pilon, 2011) are sensitive to superoxide, as reviewed elsewhere (Py et al., 2011). In both plants and animals, ROS can damage the Fe–S cluster of aconitase, an important participant of the tricarboxylic acid cycle (Verniquet et al., 1991; Gardner and Fridovich, 1991). It was recently demonstrated that selenite-induced superoxide decreased aconitase activity and levels of tricarboxylic acid cycle metabolites in *Brassica napus* (Dimkovikj and Van Hoewyk, 2014). Additionally, the Fe–S cluster in isopropylmalate dehydratase, an Fe–S protein involved in branched-chain amino acid metabolism, is also sensitive to copper-induced oxidative stress (Macomber and Imlay, 2009).

The effects of superoxide on a chloroplastic Fe–S protein have not been examined. Some chloroplastic Fe–S proteins mediate electron transport during the light reactions (Balk and Pilon, 2011). Fe–S clusters found in the cytochrome b_6f complex, photosystem I, and ferredoxin (Fd) are vital for plant development and photosynthesis (Van Hoewyk et al., 2007). Fd mediates the reduction of $NADP^+$ to NADPH. Knockout of isoform Fd2 resulted in growth impairment and ROS accumulation (Voss et al., 2008).

Numerous abiotic stressors result in superoxide accumulation (Mittler, 2002). For example, inorganic Se induces ROS accumulation and has been reported to decrease efficiency of photosystem II in Arabidopsis (Grant et al., 2011), wheat (Łabanowska et al., 2012) and *Stanleya albescens* (Freeman et al., 2010). The exact cellular mechanism is not clear, but if superoxide also damages the chloroplastic Fe–S clusters, this would likely diminish photosynthetic capacity. We reasoned that since (*i*) selenate is likely reduced to selenite in chloroplasts and if (*ii*) the non-enzymatic reduction of selenite yields superoxide, then it would potentially damage chloroplastic proteins that contain an Fe–S cluster. To test this hypothesis, the integrity of the Fe–S cluster of Fd was analyzed in a reaction containing selenite and GSH. We additionally examined if Arabidopsis plants with a mutation in SiR had altered selenite tolerance and selenium accumulation.

2. Methods

2.1. Plant selenium toxicity and elemental analysis

Seeds of SiR mutants plants used in this study were obtained as SIR KD1T seeds (Yarmolinsky et al., 2013) and *sir1-1* seeds (Khan et al., 2010), and separately compared to Columbia ecotype in the same genetic background. Plants were grown in a growth chamber (150 μE, 16 h light/8 h dark cycle, 24 C) on agar plates containing 1% sucrose and 0.5 strength Murashige and Skoog media consisting of 2.5 mM KNO_3, 25 μM FeNa-EDTA, 1 mM KH_2PO_4, 1 mMKH_2PO_4, 1 mM $Ca(NO_3)_2$.4H2O, 35 μM H_3BO_3, 7 μM $MnCl_2$, 0.25 μM $CuSO_4$, 2 mM $ZnSO_4$, and 0.4 μM $Na_2MoO_4 \cdot 2H_2O$ (Murashige and Skoog, 1962). To test the effect of selenite, agar media plates contained either 0 or 15 μM sodium selenite, a concentration known to induce toxicity (Tamaoki et al., 2008). To confirm selenite toxicity at the above-mentioned concentration, plants ($n = 20–30$) were grown with and without selenite. Selenite tolerance was determined by measuring root length in the WT and mutant plants after 14 days of growth on vertical plates. To determine elemental content, plants were grown for 21 d on horizontal agar plates; this longer time point was selected in order to obtain enough for elemental analysis. Four biological replicates per treatment consisting of several pooled plants each were rinsed and dried, and then acid digested prior to ICP-OES analysis. Elemental analysis was carried out as described before (Van Hoewyk et al., 2007; Pilon Smits et al., 1999). This included appropriate quality assurance and control, by means of National Institute of Standards and Technology standards for all elements, and a quality control checked every 15 samples. All statistical analyses (ANOVA and Student's t tests) were performed using the Kaleida-graph software package (Synergy Software).

2.2. Plant stress-induced phenotype measurements in sir1-1 plants

Total GSH content, including the pool of reduced and oxidized glutathione (GSSG), was estimated spectrophotometrically at A_{412} using Ellman's Reagent, as previously described (Grant et al., 2011). Reduced GSH was estimated as the difference between total GSH and GSSG in five individual plants. The ratio of variable and maximal Chlorophyll fluorescence (F_V/F_M), which represents the maximum photochemical efficiency of photosystem II, was measured in 25–30 dark-adapted plants using a hand-held chlorophyll fluorimeter (Photon System Instruments; Bratislava, Czech Republic) and calculated as described previously (Maxwell and Johnson, 2000).

2.3. Selenite and superoxide measurements

Ten micrograms of Fd, purified as previously described (Pilon et al., 1992; Ye et al., 2005), was incubated in a 1 mL volume containing 50 mM tricine/KOH buffer (pH 7.6), +/− 1 mM GSH, and+/− 0.1 mM sodium selenite, as described in Table 2. After a 2 h incubation at room temperature, the sample was centrifuged and the

supernatant was filtered through an Amicon Ultra-15 10 kDa MWCO (molecular weight cut off) filter. Fd was trapped on the filter, and the filtered fluid was used in subsequent analyses of selenite, superoxide, and GSH.

Selenite was measured based on a modification of the procedure according to Kessi et al. (1999). Twenty microliters of filtered fluid were added to a glass tube containing 1 ml of 0.1 M HCl, 0.05 ml of 0.1 M EDTA, 0.05 ml of 0.1 M NaF, and 0.05 ml of 0.1 M disodium oxalate. Afterwards, 0.25 ml of 0.1% 2,3-diaminonaphthalene in 0.1 M HCl was added. The solution was incubated at 40 °C for 40 min. Selenium–2,3-diaminonaphthalene was extracted with 0.6 ml of cyclohexane, vigorously mixed, and finally centrifuged for 10 min at 3000 × *g*. Levels of selenite are reported as the absorbance of the organic phase at 377 nm. Reduced GSH was measured as described above, as is reported as the absorbance of samples at 412 nm.

The production of superoxide was estimated by the reduction of nitroblue tetrazolium, which produces formazan and absorbs at 560 nm (Misra, 1974). In a 1 mL solution containing 100 mM Tris/HCl (pH 9) and 0.1 mM nitroblue tetrazolium, 100 μL of the elutant from the reactions above was mixed and incubated for 10 min at room temperature. Samples were immediately vortexed before analysis. Relative levels of superoxide were reported at A_{560}.

2.4. Spectral analysis of Fd

Additional analysis of Fd was performed in the reaction described above (+/−GSH and+/−selenite), except that the reactions were allowed to incubate for various time periods (0, 2, 4, 8, and 16 h). Recovery of pure Fd from the 10 kDa MWCO filter removed contaminants that potentially would interfere with the spectral analysis of Fd. The recovery of Fd (94–97%) was confirmed using the Bradford Assay. UV/Vis absorbance spectra (A_{260} to A_{600}) were measured using 5 μg of Fd. Integrity of Fd's 2Fe–2S cluster Fd was measured at each time point as the ratio of A_{420}:A_{260} as previously described (Yocum et al., 1975). The size of the Fe–S cluster peak was measured as the difference between A_{420} and A_{395}.

2.5. Activity assay and electrophoresis

Fd was incubated in reactions 1–4 (see Table 2) and then recovered as described above. Activity was estimated based on its ability to reduce cytochrome *c* using a modified procedure (Green et al., 1991). In a 1 mL reaction containing 50 mM Tris/HCl (pH 7.6), 0.25 mM NADPH, 0.001 units of Fd-NADP reductase (Sigma Aldrich), and 0.5 mM cytochrome *c*, 20 μg of Fd was added and incubated for 5 min. Absorbance at 550 nm was recorded every thirty seconds, and relative cytochrome *c* reduction was corrected for controlled reactions performed in the absence of Fd-NADP reductase.

After incubating for 16 h in reactions 1–4, 20 μg of Fd was resolved under non-denaturing conditions on a 15% PAGE gel. Gels were stained for total protein with Coomassie Brilliant Blue, and the levels of apo-Fd were estimated using the software Image-J by measuring the intensity of the bands running above holo-Fd.

3. Results

3.1. Knockdown of SiR does not affect Se toxicity or accumulation

To determine the importance of SiR for selenite tolerance, previously characterized *Arabidopsis thaliana* plants (SIR KD1T) with a 37% decrease in SiR activity were obtained (Yarmolinsky et al., 2013), and compared to wildtype (WT) plants in the same genetic background (ecotype Columbia). There was no difference between the root lengths of WT and SIR KDT1 plants after 14 days of growth on MS media plates lacking selenite (Fig. 1a), nor on the same medium supplemented with 15 μM selenite (Fig. 1b). Compared to control media, root length decreased nearly two-fold for both plant genotypes when grown on media supplemented with 15 μM selenite, demonstrating that this selenite concentration was toxic. Thus, selenite tolerance was not different between WT and SIR KDT1 plants.

The elemental content of selenite-treated WT and SIR KDT1 plants was analyzed to determine whether impairment of SiR altered the tissue concentration of Se or of essential nutrients. The tissue levels of Se were not affected in the KDT1 mutants. Furthermore, there were no differences between WT and SIR KDT1 in the concentration of macronutrients calcium, magnesium, and sulfur or trace elements iron, copper, and manganese in plants grown on media with or without selenite (Table 1). Thus, decreased SiR activity does not affect Se accumulation in Arabidopsis.

In a second approach to test the importance of SiR for selenite tolerance, another characterized SiR mutant (*sir1-1*) was obtained (Khan et al., 2010) and separately studied. SiR activity in these knockdown plants was reduced by almost 80%. WT and *sir1-1* plants (Columbia ecotype) exhibited the same root length when challenged with selenite (Fig. 2A), in agreement with SIR KDT1. There were no visible signs of chlorosis when challenged with selenite. However, when chlorophyll fluorescence was analyzed to determine if the mutants had photosynthetic impairments, Fv/Fm values, which represent the maximum capacity of photosystem II in dark-adapted plants, decreased when plants were grown on Se compared to control media. The Fv/Fm values did not differ between WT and *sir1-1* plants grown either with or without Se (Fig. 2B). Thus, the SiR mutants did not show evidence of altered

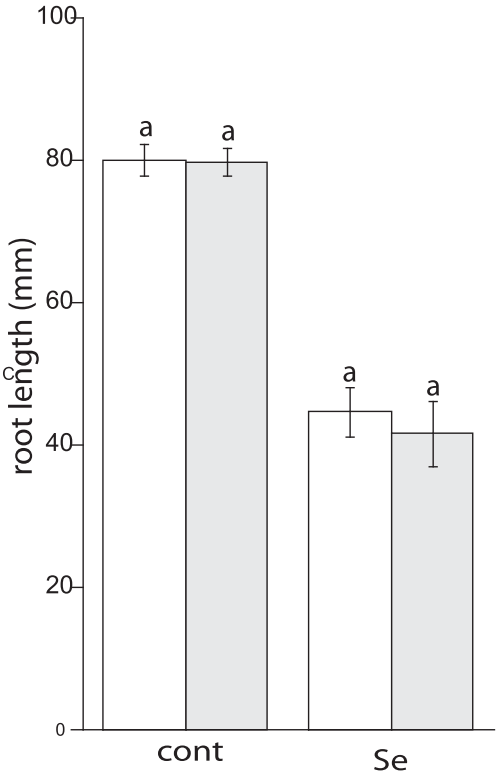

Fig. 1. Selenite tolerance in WT (white bars) and SiR KD1T (shaded bars) Arabidopsis plants grown on MS media with or without 15 μM selenite for 14 days. Results shown are the mean (n = 20–30 seedlings) and standard error. Different letters above bars denote significant differences between treatment means ($p < 0.05$). WT-wildtype.

Table 1
Elemental content (mg kg^{-1} FW) in WT and SiR KD1T Arabidopsis plants grown on control media and media with selenite for 21 d. Results shown are the mean and standard error of four independently pooled samples. Lowercase letters represent a significant difference among plants between each treatment ($p < 0.05$). Gray represents a significant difference in elemental content in selenite-treated samples. WT-wildtype. FW-fresh weight.

	WT	SiR KD1T	WT + selenite	SiR KD1T + selenite
Ca	6565 (243)[a]	6303 (136)[a]	5138 (228)[b]	4830 (257)[b]
Cu	8.2 (2.7)[ab]	6.8 (1.7)[a]	8.7 (4.7)[ab]	11.1 (2.1)[b]
Fe	248 (27)[a]	255 (17)[a]	335 (30)[b]	370 (45)[b]
Mg	1962 (67)[a]	1846 (135)[a]	1607 (147)[b]	1582 (185) [b]
Mn	263 (11)[a]	256 (3)[a]	211 (7)[b]	200 (5)[b]
S	6645 (145)[a]	6350 (357)[a]	6301 (394)[a]	6557 (431)[a]
Se	13 (2)[a]	20 (14)[a]	156 (5)[b]	157 (4)[b]

in the mixture (Table 2), indicating that these two reactants were quickly consumed in the reaction, as reported earlier (Kessi and Hanselmann, 2004). The reaction of GSH and selenite produced superoxide as expected, which did not accumulate in other mixtures: reaction number 1 (Fd); reaction number 2 (Fd + GSH); reaction number 3 (Fd + selenite). Additional experiments focused on the consequences of superoxide generated in mixture 4 (reaction with both GSH and selenite) on the intactness of the Fe–S cluster in Fd. The absorbance spectra of plant holoFd-including spinach Fd usedin this study-is characterized by shoulders at 420 and 330 nm (Tagawa and Arnon, 1962; Ceccoli et al., 2011). The A_{330} peak is ascribed to the vibration between the cluster's Fe atoms and its cysteine ligand in the protein, and the A_{420} peak is due to vibration

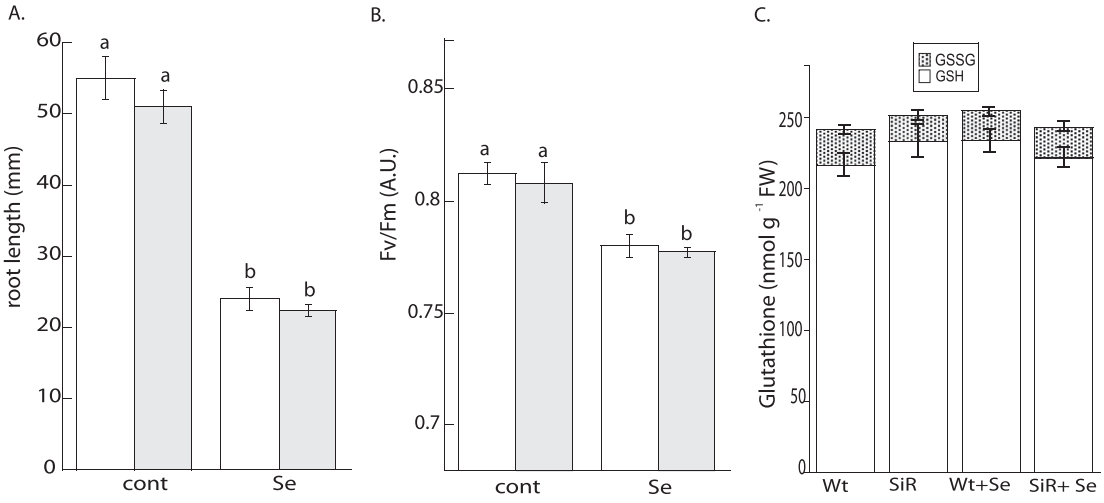

Fig. 2. Characterization of *sir1-1* Arabidopsis plants grown on MS media with or without 15 μM selenite for 10 days. (A) Root length and (B) Fv/Fm values in WT (white bars) and *sir1-1* (shaded bars) plants. (C) Levels of reduced GSH and oxidized glutathione (GSSG) in WT and *sir1-1* plants. Results shown are the mean and standard error. Different letters above bars denote significantly different means ($P < 0.05$). GSH- reduced gluthatione, GSSG-oxidized glutathione, WT-wildtype.

selenite tolerance.

Lastly, we deemed it important to measure the concentration of GSH, an anti-oxidant that also represents the majority of non-protein thiols in plants. There was no difference in GSH between WT and *sir1-1* plants, either grown with selenite (Fig. 2C) or without as previously reported (Khan et al., 2010). In summary, there was no distinguishable phenotypic difference between *sir1-1* and WT plants when grown on selenite.

3.2. Non-enzymatic reduction of selenite impairs Fd

If selenite reduction is not primarily mediated by SiR, and instead happens non-enzymatically *via* GSH, the resulting products are selenodiglutathione and superoxide (Kessi and Hanselmann, 2004). The effects of this superoxide produced as a result of selenite reduction in chloroplasts deserved further investigation. Since superoxide is known to damage the Fe–S clusters of mitochondrial and cytosolic proteins, it likely can also damage the Fe–S cluster of chloroplastic proteins. Therefore, further experimentation addressed the question whether GSH-mediated selenite reduction damages the Fe–S cluster of Fd and impairs its activity. Fd was isolated from fresh spinach plants rather than Arabidopsis to increase yield of the protein, and then used in subsequent *in vitro* assays. Preliminary experiments verified that reaction mixture number 4 (containing Fd, reduced GSH, and selenite) generated superoxide after 2 h. Levels of selenite and reduced GSH decreased between the Fe and the inorganic S in the 2Fe–2S cluster (Morimoto et al., 2002). In a solution containing selenite and GSH, Fd's absorption spectra were visibly distinct after 16 h compared to Fd in control reactions (Fig. 3A). Notably, there was increased absorbance in the UV range, and loss of absorbance at A_{330} and A_{420}, indicating damage to the Fe–S cluster. Pure Fd in spinach has a A_{420}/A_{276} ratio of 0.49–0.47 (Schürmann et al., 1970; Yocum et al., 1975). In the reaction with selenite and GSH, the purity of Fd began to decrease after 2 h, and after 16 h the A_{420}/A_{276} ratio was nearly 40% lower compared to controls (Fig. 3B). The integrity of the Fd's Fe–S cluster was analyzed by monitoring the absorbance at 420 and 395 nm. After 12 h, the size of the peak at A_{420} decreased by 50% compared to control reactions, indicating damage to the Fe–S cluster in the presence of selenite and GSH (Fig. 3C). Damage to Fe–S clusters result in its removal from the holoprotein to yield an apoprotein. To gauge the formation of apo-Fd resulting from its incubation with GSH + selenite after 16 h, proteins were analyzed *via* PAGE under non-denaturing conditions. Pure holo-Fd ran as a single band with high mobility (Fig. 4). Fd that incubated with selenite + GSH produced four or five spurious bands that represent apo-Fd, which is known to migrate more slowly than holo-Fd on a nondenaturing gel (Takahashi et al., 1986). These data further confirm the loss of absorbance at 420 nm, indicating that GSH-mediated reduction damages the Fe–S cluster of Fd. Intriguingly, Fd that reacted with selenite also produced two bands that migrated slower than holo-Fd. However, the intensity of the apo-Fd

Table 2
Relative levels of reduced GSH, selenite, and superoxide in reactions 1–4 after 2 h. Reaction with GSH and selenite consumed reduced GSH and selenite, and produced superoxide. Results shown are the absorbance of each sample, and represent 5–7 independently performed experiments. GSH-glutathione, Se-selenite, O_2^- – superoxide. Lowercase letters represent a significant difference between reactions ($p < 0.05$).

Reaction	Fd (10 μg)	GSH (1 mM)	Se (0.1 mM)	GSH (A_{412}nm)	Selenite (A_{377} nm)	O_2^- (A_{560} nm)
1	+	–	–	0	0.01 (0.01)[a]	0.03 (0.01)[a]
2	+	+	–	0.41 (0.05)[a]	0.05 (0.03)[ab]	0.02 (0.01)[a]
3	+	–	+	0	0.57 (0.04)[c]	0.07 (0.02)[b]
4	+	+	+	0.11 (.02)[b]	0.07 (0.02)[b]	0.86 (0.1)[c]

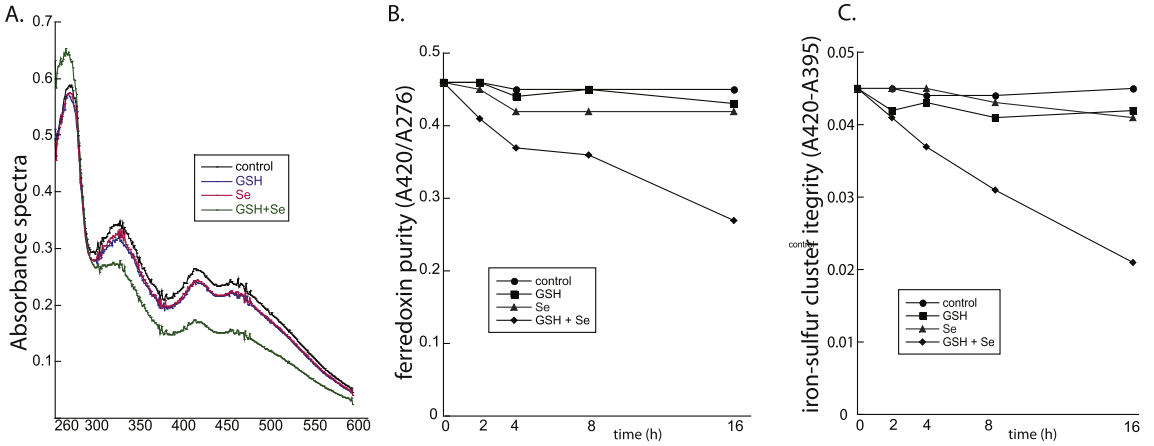

Fig. 3. Absorption spectra and properties of Fd in a reaction containing+/−1 mM GSH and+/−0.1 mM selenite. Fd incubated in four conditions described in Table 2 for 0, 2, 4, 8, and 16 h. (A) Absorption spectra after a 16 h incubation in reactions 1–4. (B) Purity of Fd as determined by the A_{420}:A_{276} ratio. (C) Integrity of the Fe–S cluster of Fd as determined by the absorbance difference at A_{420} and A_{395}. All data are representative representations for 5–7 independently performed experiments. Fd-ferredoxin, GSH- glutathione, Se-selenite.

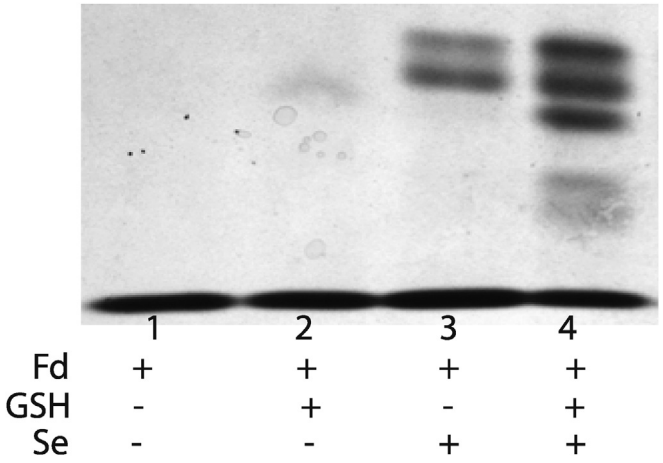

Fig. 4. Non-denaturing polyacrylamide gel electrophoresis (PAGE) showing ferredoxin after 16 h in reactions 1–4 as described in Table 2. Ferredoxin was stained with Coomassie Brilliant Blue on a 15% gel, and is representative of three other independent experiments. Numbers above lanes 3 and 4 correspond to band intensity relative to lane 3. Fd-ferredoxin.

bands in the reaction treated with selenite + GSH was 3-fold more than the sample treated with just selenite. Lastly, the effect of superoxide on the activity of Fd was assayed by determining its ability to reduce cytochrome *c*. After 8 and 16 h, there was a 12% and 41% decrease in Fd activity in the GSH + selenite sample (Fig. 5). The superoxide-induced decrease in activity coincides with impairment of the Fe–S cluster and the protein's denaturation, as judged by the formation of apo-Fd.

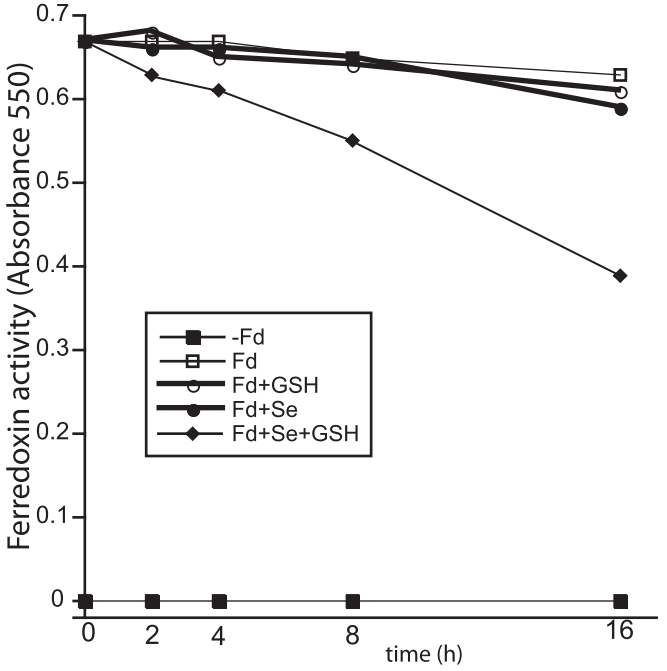

Fig. 5. Ferredoxin activity, as determined by its ability to reduce cytochrome *c* in a reaction containing NADPH and ferredoxin-NADP reductase. Activity at the indicated time points is reported as A_{550} in reactions 1–4 as described in Table 2. Data are representative of five independent experiments.

4. Discussion

Arabidopsis plants with decreased SiR activity were previously

shown to be susceptible to sulfite (Yarmolinsky et al., 2013) and cadmium (Khan et al., 2010) toxicity. In contrast, these same plants did not show any differences in growth, chlorophyll fluorescence or Se accumulation when challenged with a toxic concentration of selenite. This finding suggests that SiR is not a rate-limiting enzyme for Se assimilation, or may not even be involved in this process *in vivo*, and agree with a previous study suggesting that SiR does not likely have selenite reductase activity (Ng and Anderson, 1979).

Although a plant-specific selenite reductase remains elusive, studies in other organisms strongly suggest that selenite reduction might be facilitated by a wide-range of alternative enzymes. For example, selenite can be reduced in a NADPH-dependent manner by thioredoxin in calf cells (Kumar et al., 1992) and *E. coli* (Hunter, 2014). Additionally, selenite reduction in human cells can occur *via* at least two different glutaredoxins (Wallenberg et al., 2010). In microbial organisms, selenite has also been reported to be a substrate for various oxidoreductases, including nitrite reductase (Basaglia et al., 2007), fumarate reductase (Li et al., 2014), and glutathione reductase (Ni et al., 2015). Collectively, these data point to the possibility that selenite reduction in plants can proceed enzymatically, even if it does not involve SiR.

Additionally, selenite can be reduced non-enzymatically by GSH to yield two products: selenodiglutathione and superoxide (Seko et al., 1989; Spallholz, 1994; Kessi and Hanselmann, 2004; Chen et al., 2007). In the presence of GSH reductase and NADPH, selenodigluthatione is converted into selenide, and this product is further metabolized into selenocysteine *via* cysteine synthase (Ng and Anderson, 1979). The other product-superoxide- is a ROS. Data presented in this study indicate that Fd is susceptible to damage by superoxide generated from a reaction with 0.1 mM selenite and 1 mM GSH, which is near the reported 1.2 mM concentration of GSH in the chloroplast (Koffler et al., 2011). UV/Vis spectroscopy indicated a time-dependent impairment of the Fe–S cluster of Fd, as determined by a decrease in the A_{420}/A_{276} ratio. Superoxide increased the absorbance of Fd at 276 nm, and had the opposite effect at 420 nm; these data are in agreement with another study that investigated the unfolding of Fd (Bandyopadhyay and Sonawat, 2000). Impairment of the Fe–S cluster coincided with both decreased activity and the formation of apo-Fd. Taken together, our data point to the ability of superoxide to damage Fd by altering the integrity of its Fe–S cluster.

A variety of stressors are known to decrease protein levels of Fd in plants (Ceccoli et al., 2011; Tognetti et al., 2006), which could be explained by at least two different mechanisms. Supplementation with the antioxidant GSH in Arabidopsis plants can overcome oxidative stress during Fe deficiency and restore levels of Fd (Rameriz et al., 2013); these data suggest that ROS are directly impairing Fd, a conclusion that coincides with the observations made in our study. Secondly, transfer of an Fe–S cluster to Fd can be mediated by glutaredoxin and is GSH-dependent (Wang et al., 2012). Glutathione levels often decrease during severe oxidative stress (Mittler, 2002), and the depletion of GSH could directly impede formation of holo-Fd.

Oxidatively-damaged Fe–S proteins in *E. coli* result in the accumulation of free intracellular Fe (Keyer and Imlay, 1996; Touati, 2000). Although intracellular Fe was not measured in our study, the total leaf concentration of Fe increased nearly 40% when plants were grown on selenite; no other element increased when challenged with Se. In agreement with our observation, rice seedlings treated with ROS-inducing methyl viologen also enhanced leaf Fe concentration, and was associated with up-regulation of transcripts involved in Fe–S cluster assembly; induction of these genes might be a consequence of Fe–S damage (Liang et al., 2014). Thus, it is possible that the increase in total Fe in plants experiencing oxidative stress stems from damage to Fe–S clusters and the release of Fe from proteins, triggering enhanced Fe uptake into the plants. However, this has yet to be biochemically examined *in planta*.

The damaging effects of ROS on Fe–S clusters now include Fd, and might be extended to other chloroplastic proteins that harbor an Fe–S cluster. Under this scenario (Fig. 6), photosynthetic

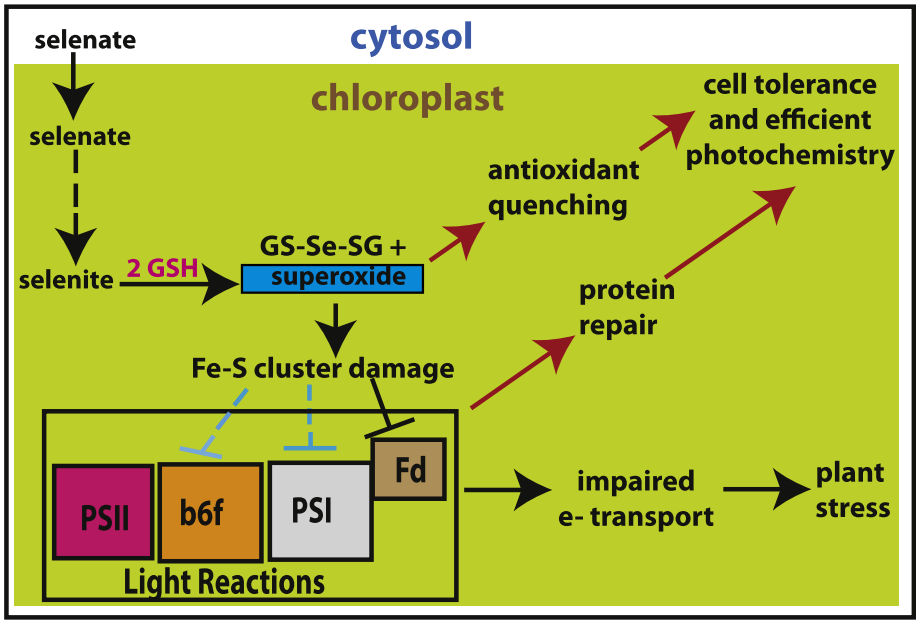

Fig. 6. Schematic diagram depicting how superoxide generated from the glutathione-mediated reduction of selenite might cause plant stress if a proper stress response (red arrows) is not mounted. Selenate is reduced to selenite in plastids *via* the sulfate assimilation pathway (Zhu et al., 2009). Selenite is further reduced by GSH, which generates superoxide as a byproduct (Kessi and Hanselmann, 2004). The superoxide in turn damages the Fe–S cluster and folding of ferredoxin (Fig. 3). The photosynthetic electron transport chain is dependent upon Fe–S clusters, and its impairment decreases photochemistry and causes plant stress (Van Hoewyk et al., 2007). Dotted black lines represent steps in the sulfate assimilation pathway. Dotted blue lines represent possible damage to other Fe–S proteins caused by superoxide, but this has yet to be experimentally determined. GS-Se-SG-selenodiglutathione, SODs-superoxide dismutases. (For interpretation of the references to colour in this figure legend, the reader is referred to the web version of this article.)

impairment would be anticipated, because the electron transport chain is also dependent upon Fe–S proteins found in the cytochrome b_6/f complex and photosystem I (Balk and Pilon, 2011). Superoxide's damaging effect of Fe–S clusters is especially detrimental if the Fe–S proteins cannot be repaired or if the cells' antioxidant capacity to quench free radicals is compromised or over-whelmed, which frequently occurs during abiotic stress. For example, an *E. coli* mutant with defects in superoxide dismutases (SODs) are especially vulnerable to Fe–S cluster damage during oxidative stress (Jang and Imlay, 2007). However, in plants, the role of chloroplastic SODs in mitigating photoprotection during oxidative stress is more ambiguous (Pilon et al., 2011); for example, Arabidopsis plants with decreased levels of plastidal copper/zinc SOD are not sensitive to high light or methyl viologen, but intriguingly have reduced growth when treated with selenium (Cohu et al., 2009). It should also be noted that toxic levels of Se result in the accumulation of ROS, and can also decrease photosynthetic electron transport (Van Hoewyk, 2013). This raises the question if Se-induced photochemical inhibition is partially attributable to Fe–S cluster damage. In addition to Se, our data may provide a mechanism to account for decreased photosynthesis that often occurs during a variety of abiotic stresses.

Author contributions

DVH conceived the project. DVH, MS, and EAPS designed experiments. BF, DVH, EAPS, and DY performed the experiments and data analysis. DY generated the SiRKD1 plants, and SAG and MP isolated ferredoxin. DVH wrote the manuscript, but was assisted by all coauthors who helped edit and prepare the paper.

Acknowledgements

DVH thanks Ali Ergul and Aykut Ozkul for shared facilities during the preparation of this manuscript. DVH thanks Markus Wirtz for providing the *sir1-1* plants. This project was supported from the NSF-RUI Program (MCB-1244009) awarded to DVH.

References

Balk, J., Pilon, M., 2011. Ancient and essential: the assembly of iron-sulfur clusters in plants. Trends Plant Sci. 16, 18–26.
Bandyopadhyay, A.K., Sonawat, H.M., 2000. Salt dependent stability and unfolding of [Fe2-S2] ferredoxin of Halobacterium salinarum: spectroscopic investigations. Biophys. J. 79, 501–510.
Basaglia, M., Toffanin, A., Baldan, E., Bottegal, M., Shapleigh, J.P., Casella, S., 2007. Selenite-reducing capacity of the copper-containing nitrite reductase of *Rhizobium sullae*. FEMS Microbiol. Lett. 269, 124–130.
Ceccoli, R.D., Blanco, N.E., Medina, M., Carrillo, N., 2011. Stress response of transgenic tobacco plants expressing a cyanobacterial ferredoxin in chloroplasts. Plant Mol. Biol. 76, 535–544.
Chen, J.J., Boylan, L.M., Wu, C.K., Spallholz, J.E., 2007. Oxidation of glutathione and superoxide generation by inorganic and organic selenium compounds. Biofactors 31, 55–66.
Cohu, C.M., Abdel-Ghany, S.E., Reynolds, K.A., Onofrio, A.M., Bodecker, J.R., Kimbrel, J.A., Niyogi, K.K., Pilon, M., 2009. Copper delivery by the copper chaperone for chloroplast and cytosolic copper/zinc-superoxide dismutases: regulation and unexpected phenotypes in an Arabidopsis mutant. Mol. plant 2, 1336–1350.
Dilworth, G.L., Bandurski, R.S., 1977. Activation of selenate by adenosine 5′-triphosphate sulphurylase from *Saccharomyces cerevisiae*. Biochem. J. 163, 521–529.
Dimkovikj, A., Van Hoewyk, D., 2014. Selenite activates the alternative oxidase pathway and alters primary metabolism in Brassica napus roots: evidence of a mitochondrial stress response. BMC Plant Biol. 14, 259. http://dx.doi.org/10.1186/s12870-014-0259-6.
El Kassis, E., Cathala, N., Rouached, H., et al., 2007. Characterization of a selenate-resistant Arabidopsis mutant: root growth as a potential target for selenate toxicity. Plant Physiol. 143, 1231–1241.
Freeman, J.L., Tamaoki, M., Stushnoff, C., et al., 2010. Molecular mechanisms of selenium tolerance and hyperaccumulation in *Stanleya pinnata*. Plant Physiol. 153, 1630–1652.
Gardner, P.R., Fridovich, I., 1991. Superoxide sensitivity of the *Escherichia coli* aconitase. J. Biol. Chem. 266, 19328–19333.
Grant, K., Carey, N.M., Mendoza, M., et al., 2011. Adenosine 5-phosphosulfate reductase (APR2) mutation in Arabidopsis implicates glutathione deficiency in selenate toxicity. Biochem. J. 438, 325–335.
Green, L.S., Yee, B.C., Buchanan, B.B., Kamide, K., Sanada, Y., Wada, K., 1991. Ferredoxin and ferredoxin-NADP reductase from photosynthetic and non-photosynthetic tissues of tomato. Plant physiol. 96, 1207–1213.
Hunter, W.J., 2014. A Rhizobium selenitireducens protein showing selenite reductase activity. Curr. Microbiol. 68, 311–316.
Jang, S., Imlay, J.A., 2007. Micromolar intracellular hydrogen peroxide disrupts metabolism by damaging iron-sulfur enzymes. J. Biol. Chem. 282, 929–937.
Kessi, J., 2006. Enzymic systems proposed to be involved in the dissimilatory reduction of selenite in the purple non-sulfur bacteria *Rhodospirillum rubrum* and *Rhodobacter capsulatus*. Microbiology 152, 731–743.
Kessi, J., Hanselmann, K.W., 2004. Similarities between the abiotic reduction of selenite with glutathione and the dissimilatory reaction mediated by *Rhodospirillum rubrum* and *Escherichia coli*. J. Biol. Chem. 279, 50662–50669.
Kessi, J., Ramuz, M., Wehrli, E., Spycher, M., Bachofen, R., 1999. Reduction of selenite and detoxification of elemental selenium by the Phototrophic BacteriumRhodospirillum rubrum. Appl. Environ. Microbiol. 65, 4734–4740.
Keyer, K., Imlay, J.A., 1996. Superoxide accelerates DNA damage by elevating free-iron levels. Proc. Natl. Acad. Sci. 93, 13635–13640.
Khan, M.S., Haas, F.H., Samami, A.A., Gholami, A.M., Bauer, A., Fellenberg, K., Reichelt, M., Hänsch, R., Mendel, R.R., Meyer, A.J., Wirtz, M., 2010. Sulfite reductase defines a newly discovered bottleneck for assimilatory sulfate reduction and is essential for growth and development in Arabidopsis thaliana. Plant Cell 22, 1216–1231.
Kumar, S., Bjornsted, M., Holmgren, A., 1992. Selenite is a substrate for calf thymus thioredoxin reductase and thioredoxin and elicits a large non-stoichiometric oxidation of NADPH in the presence of oxygen. Eur. J. Biochem. 207, 435–439.
Li, D.B., Cheng, Y.Y., Wu, C., Li, W.W., Li, N., Yang, Z.C., Tong, Z.H., Yu, H.Q., 2014. Selenite Reduction by *Shewanella Oneidensis* MR-1 Is Mediated by Fumarate Reductase in Periplasm. Scientific Reports. 2014 Jan 17, p. 4.
Liang, X., Qin, L., Liu, P., Wang, M., Ye, H., 2014. Genes for iron–sulphur cluster assembly are targets of abiotic stress in rice, *Oryza sativa*. Plant, Cell & Environ. 37, 780–794.
Macomber, L., Imlay, J.A., 2009. The iron-sulfur clusters of dehydratases are primary intracellular targets of copper toxicity. In: Proceedings of the National Academy of Sciences, USA, vol. 106, pp. 8344–8349.
Maxwell, K., Johnson, G.N., 2000. Chlorophyll fluorescence – a practical guide. J. Exp. Bot. 359, 659–668.
Misra, H.P., 1974. Generation of superoxide free radical during the autoxidation of thiols. J. Biol. Chem. 249, 2151–2155.
Mittler, R., 2002. Oxidative stress, antioxidants and stress tolerance. Trends Plant Sci. 7, 405–410.
Morimoto, K., Nishio, K., Nakai, M., 2002. Identification of a novel prokaryotic HEAT-repeats-containing protein which interacts with a cyanobacterial IscA homolog. FEBS Lett. 519, 123–127.
Murashige, T., Skoog, F., 1962. Revised medium for rapid growth and bioassays with tobacco tissue culture. Physiol. Plant 15, 473–497.
Ng, B.H., Anderson, J.W., 1979. Light-dependent incorporation of selenite and sulphite into selenocysteine and cysteine by isolated pea chloroplasts. Phytochemistry 18, 573–580.
Ni, T.W., Staicu, L.C., Nemeth, R.S., Schwartz, C.L., Crawford, D., Seligman, J.D., Hunter, W.J., Pilon-Smits, E.A., Ackerson, C.J., 2015. Progress toward clonable inorganic nanoparticles. Nanoscale 7, 17320–17327.
Pilon, M., Rietveld, A.G., Weisbeek, P.J., De Kruijff, B., 1992. Secondary structure and folding of a functional chloroplast precursor protein. J. Biol. Chem. 267, 19907–19913.
Pilon, M., Ravet, K., Tapken, W., 2011. The biogenesis and physiological function of chloroplast superoxide dismutases. Biochim. et Biophys. Acta (BBA)-Bioenergetics 1807, 989–998.
Pilon-Smits, E.A.H., Quinn, C.F., 2010. Selenium metabolism in plants. In: Hell, R., Mendel, R. (Eds.), Cell Biology of Metal and Nutrients. Springer, Berlin, pp. 225–241.
Pilon-Smits, E.A., Hwang, S., Lytle, C.M., Zhu, Y., Tai, J.C., Bravo, R.C., Chen, Y., Leustek, T., Terry, N., 1999. Overexpression of ATP sulfurylase in Indian mustard leads to increased selenate uptake, reduction, and tolerance. Plant Physiol. 119, 123–132.
Py, B., Moreau, P.L., Barras, F., 2011. Fe–S clusters, fragile sentinels of the cell. Curr. Opin. Microbiol. 14, 218–223.
Ramírez, L., Bartoli, C.G., Lamattina, L., 2013. Glutathione and ascorbic acid protect Arabidopsis plants against detrimental effects of iron deficiency. J. Exp. Bot. 64, 3169–3178.
Rayman, M.P., 2000. The importance of selenium to human health. Lancet 356, 233–241.
Schürmann, P., Buchanan, B.B., Matsubara, H., 1970. Ferredoxin from fern and amaranthus: two diverse plants with similar ferredoxins. Biochim. et Biophys. Acta (BBA)-Bioenergetics 223, 450–462.
Seko, Y., Saito, T., Kitahara, J., Imura, N., 1989. Active oxygen generation by the reaction of s elenite with reduced glutathione in vitro. In: Wendel, A. (Ed.), Proceedings of the Fourth International Symposium on Selenium in Biology and Medicine. Heidelburg: Springer-Verlag, pp. 70–73.
Sors, T.G., Ellis, D.R., Na, G.N., et al., 2005. Analysis of sulfur and selenium

assimilation in Astragalus plants with varying capacities to accumulate selenium. Plant J. 42, 785–797.
Spallholz, J.E., 1994. On the nature of selenium toxicity and carcinostatic activity. Free Radic. Biol. Med. 17, 45–64.
Tagawa, K., Arnon, D.I., 1962. Ferredoxins as electron carriers in photosynthesis and in the biological production and consumption of hydrogen gas. Nature 195, 537–543.
Takahashi, Y., Mitsui, A., Hase, T., Matsubara, H., 1986. Formation of the iron-sulfur cluster of ferredoxin in isolated chloroplasts. In: Proceedings of the National Academy of Sciences, USA, vol. 83, pp. 2434–2437.
Tamaoki, M., Freeman, J.L., Pilon-Smits, E.A., 2008. Cooperative ethylene and jasmonic acid signaling regulates selenite resistance in Arabidopsis. Plant Physiol. 146, 1219–1230.
Tognetti, V.B., Palatnik, J.F., Fillat, M.F., Melzer, M., Hajirezaei, M.R., Valle, E.M., Carrillo, N., 2006. Functional replacement of ferredoxin by a cyanobacterial flavodoxin in tobacco confers broad-range stress tolerance. Plant Cell 18, 2035–2050.
Touati, D., 2000. Iron and oxidative stress in bacteria. Archives Biochem. Biophys. 373, 1–6.
Turner, R.J., Weiner, J.H., Taylor, D.E., 1998. Selenium metabolism in *Escherichia coli*. Biometals 11, 223–227.
Vallentine, P., Hung, C.Y., Xie, J., Van Hoewyk, D., 2014. The ubiquitin–proteasome pathway protects *Chlamydomonas reinhardtii* against selenite toxicity, but is impaired as reactive oxygen species accumulate. AoB Plants, 6:plu062.
Van Hoewyk, D., 2013. A tale of two toxicities: malformed selenoproteins and oxidative stress both contribute to selenium stress in plants. Ann. Bot. 112, 965–972.
Van Hoewyk, D., Abdel-Ghany, S.E., Cohu, C.M., Herbert, S.K., Kugrens, P., Pilon, M., Pilon- Smits, E.A., 2007. Chloroplast iron-sulfur cluster protein maturation requires the essential cysteine desulfurase CpNifS. In: Proceedings of the National Academy of Sciences, USA, vol. 104, pp. 5686–5691.
Verniquet, F., Gaillard, J., Neuburger, M., Douce, R., 1991. Rapid inactivation of plant aconitase by hydrogen peroxide. Biochem. J. 276, 643–648.
Voss, I., Koelmann, M., Wojtera, J., Holtgrefe, S., Kitzmann, C., Backhausen, J.E., Scheibe, R., 2008. Knockout of major leaf ferredoxin reveals new redox-regulatory adaptations in *Arabidopsis thaliana*. Physiol. Plant. 133, 584–598.
Wallenberg, M., Olm, E., Hebert, C., Bjornstedt, M., Fernandes, A.P., 2010. Selenium compounds are substrates for glutaredoxins: a novel pathway for selenium metabolism and a potential mechanism for selenium-mediated cytotoxicity. Biochem. J. 429, 85–93.
Wang, L., Ouyang, B., Li, Y., Feng, Y., Jacquot, J.P., Rouhier, N., Xia, B., 2012. Glutathione regulates the transfer of iron-sulfur cluster from monothiol and dithiol glutaredoxins to apo ferredoxin. Protein & Cell 3, 714–721.
Yarmolinsky, D., Brychkova, G., Fluhr, R., Sagi, M., 2013. Sulfite reductase protects plants against sulfite toxicity. Plant Physiol. 161, 725–743.
Ye, H., Garifullina, G.F., Abdel-Ghany, S.E., Zhang, L., Pilon-Smits, E.A., Pilon, M., 2005. The chloroplast NifS-like protein of *Arabidopsis thaliana* is required for iron–sulfur cluster formation in ferredoxin. Planta 220, 602–608.
Yocum, C.F., Nelson, N., Racker, E., 1975. A combined procedure for preparation of plastocyanin, ferredoxin, and CF1. Prep. Biochem. 5, 305–317.
Zhu, Y.G., Pilon-Smits, E.A., Zhao, F.J., Williams, P.N., Meharg, A.A., 2009. Selenium in higher plants: understanding mechanisms for biofortification and phytoremediation. Trends Plant Sci. 14, 436–442.
Łabanowska, M., Filek, M., Kościelniak, J., Kurdziel, M., Kuliś, E., Hartikainen, H., 2012. The effects of short-term selenium stress on Polish and Finnish wheat seedlings—EPR, enzymatic and fluorescence studies. J. Plant Physiol. 169, 275–284.